Constructing circle patterns using a new functional

Boris A. Springborn

Institut für Mathematik, Sekr. 8-5, Technische Universität Berlin, Strasse des 17. Juni 136, 10623 Berlin, Germany. *springb@math.tu-berlin.de*

1 Introduction

Ever since Thurston, in the 1980's, called attention to the close relationship between packings and patterns of circles on the one hand and conformal maps on the other [Thu], the former have become a favorite object of mathematical research. It was shown that circle packings and circle patterns can be used to approximate conformal maps [RS87, Sch97]. This opens the possibility to develop numerical methods for conformal maps that are based on the construction of circle packings or patterns. Thurston's original algorithm to construct circle patterns was developed further by Stephenson and implemented in the program `circlepack` [DS95]. There are efforts to apply the approximation of conformal maps via circle patterns in medical imaging [HBS$^+$99].

In the paper with Bobenko [BS02], we presented two new functionals for the construction of circle patterns. One belongs to Euclidean, the other to hyperbolic geometry. Building on methods that were developed by Colin de Verdière[CdV91], we used the variational approach to prove existence and uniqueness results for circle patterns. We could also clarify the relationship between our functionals and the functionals found by Colin de Verdière[CdV91], Brägger [Brä92], and Rivin [Riv94], and derive a functional which seems to be identical with Leibon's [Lei01]. For the practical construction of circle patterns, our functionals have obvious advantages over the others: They are given in closed form, whereas for Colin de Verdière's functionals only the derivatives are given in closed form. In principle, knowledge of the gradient is enough to minimize a function, but more efficient algorithms can be used if the function itself can be evaluated. Surprisingly, the evaluation of our functional is computationally not very expensive, as is shown in section 6. Moreover, the optimization of our functionals is not subject to any constraints. This is also true for Colin de Verdière's functionals, but the others require optimization under linear equality and inequality constraints.

Whereas the paper [BS02] is concerned with existence and uniqueness questions, the purpose of this paper is to give a brief but self-contained exposition of the Euclidean functional with a focus on the practical aspects. Examples of circle patterns that were constructed using the functional are presented. The last section describes how the functional can be evaluated numerically. For the sake of brevity we treat only the simplest case, circle patterns with no curvature which correspond to a cellular decomposition of the disc; and all combinatorial-topological subtleties are glossed over.

2 Circle patterns

Figure 1 shows a cellular decomposition of a topological disc and a two pat-

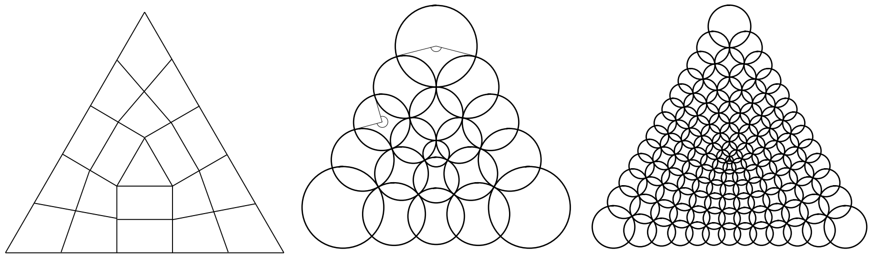

(a) (b) (c)

Fig. 1. A cellular decomposition of the disc and two circle patterns.

terns of circles. The cellular decomposition 1(a) corresponds to the pattern 1(b). The faces (2-cells) of the decomposition correspond to circles of the pattern and the vertices (0-cells) correspond to points where circles intersect. The pattern of figure 1(c) corresponds to an analogous cellular decomposition with more faces. The circle patterns are determined up to similarity by the following data.

- *The cellular decomposition*, or more precisely, its combinatorial type.
- *Intersection angles:* a function on the edges (1-cells) of the cellular decomposition prescribing the intersection angles of the circles corresponding to adjacent faces. In this example, all intersection angles are $\pi/2$.
- *Boundary conditions:* a function on the boundary faces of the cellular decomposition prescribing, for each circle, the total angle subtended by the neighboring circles. In figure 1(b), this angle is indicated for two boundary circles. In this example, it is $5\pi/6$ for the corner circles and $3\pi/2$ for the other boundary circles. The boundary conditions were chosen such that the outer intersection points lie on the sides of an equilateral triangle.

The name of Neumann was put to this type of boundary conditions by Colin de Verdière. Prescribing instead the radii of the circles on the boundary constitutes the corresponding Dirichlet problem. It may also be treated with the functional below.

We are going to show how to construct a circle pattern from the above data using a variational approach. If, in addition to the cellular surface and the intersection angles, also the radii of the circles were known, then the circle pattern could be reconstructed in the following way: Start with an arbitrary face of the cellular decomposition and place the corresponding circle somewhere in the plane. Then add cyclically and one by one the circles corresponding to the neighboring faces. Continue in the obvious fashion until all the circles are placed. If the radii are correct, the circles will fit together and the whole pattern will be reconstructed. The problem is therefore reduced to finding the correct radii. It turns out to be more convenient to use the logarithmic radii as variables. We will derive a convex function of these logarithmic radii that achieves a minimum if the radii are correct.

3 Preliminaries

Consider a triangle with sides 1 and e^x and an angle θ between them, as shown in figure 2(a). The angle between the side of unit length and the third

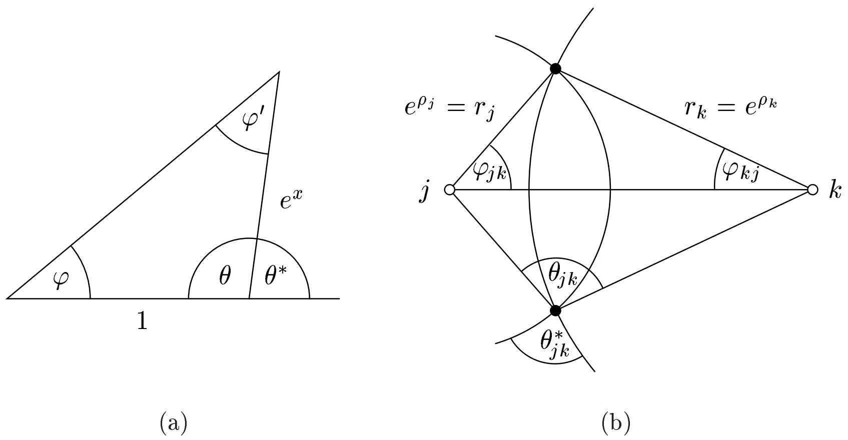

Fig. 2. Notation.

side is $\varphi = f_\theta(x)$, where

$$f_\theta(x) = \frac{1}{2i} \log \frac{1 - e^{x - i\theta}}{1 - e^{x + i\theta}}.$$

We always consider the principal branch of the logarithm function which takes values with imaginary part between $-\pi$ and π. If $\theta = \pi/2$, then $f_\theta(x) =$

arctan e^x. By rescaling the triangle, one sees that the third angle is $\varphi' = f_\theta(-x)$. Since the angles sum to π, it follows that

$$f_\theta(-x) = \theta^* - f_\theta(x), \tag{1}$$

where $\theta^* = \pi - \theta$. The derivative of f_θ is

$$f'_\theta(x) = \frac{\sin\theta}{2(\cosh x - \cos\theta)}. \tag{2}$$

It turns out that the integral is

$$\int_{-\infty}^{x} f_\theta(\xi)\, d\xi = \operatorname{Im} \operatorname{Li}_2(e^{x+i\theta}), \tag{3}$$

where Im denotes the imaginary part and Li_2 is the dilogarithm function. Inside and on the unit circle, it is defined by the power series

$$\operatorname{Li}_2(z) = \sum_{k=1}^{\infty} \frac{z^k}{k^2}. \tag{4}$$

One deduces the integral representation

$$\operatorname{Li}_2(z) = -\int_0^z \frac{\log(1-\zeta)}{\zeta}\, d\zeta, \tag{5}$$

which reveals that the power series may be analytically continued to the complex plane with a cut from 1 to ∞ along the real axis. This is the principal branch of the dilogarithm, with which we will be concerned exclusively.

4 The functional

Suppose that the intersection angles of a circle pattern are prescribed by a function θ (or equivalently $\theta^* = \pi - \theta$) on the edges of a cellular decomposition. (See figure 2(b).) The intersection angles may lie in the range $0 < \theta < \pi$. Suppose the boundary conditions are given by a positive function Φ on the boundary faces. It is convenient to extend Φ to a function on *all* the faces by assigning the value 2π to interior faces. Then the logarithmic radii $\rho = \log r$ have to satisfy the following equations. There is one equation for each face. The equation for a face j is

$$\sum_k 2 f_{\theta_{jk}}(\rho_k - \rho_j) = \Phi_j, \tag{6}$$

where the sum is taken over all faces k meeting j in an edge, and θ_{jk} denotes the value of θ on the edge between the faces j and k.

Now we define the functional $S(\rho)$. For a function ρ on the faces, let

$$
\begin{aligned}
S(\rho) = \sum_{j\circ\!\mid\!\circ k} \big(&\operatorname{Im}\operatorname{Li}_2(e^{\rho_k-\rho_j+i\theta_{jk}}) + \operatorname{Im}\operatorname{Li}_2(e^{\rho_j-\rho_k+i\theta_{jk}}) - \theta^*_{jk}(\rho_j+\rho_k)\big) \\
&+ \sum_{\circ j} \Phi_j \rho_j,
\end{aligned}
\tag{7}
$$

where the first sum is taken over all interior edges and j and k are the faces on either side. The second sum is taken over all faces j.

A function ρ on the faces satisfies equations (6) if and only if it is a critical point of S. Indeed, from equations and (1) and (3), one finds that

$$
\frac{\partial S}{\partial \rho_j} = -\sum_k 2 f_{\theta_{jk}}(\rho_k - \rho_j) + \Phi_j, \tag{8}
$$

where the sum is taken over all faces k meeting face j in an edge. Hence $\partial S/\partial\rho_j = 0$ if and only if equation (6) is satisfied.

Now, consider how the functional S behaves if all radii are scaled by a common factor. Thus, let ρ be a function on the faces, $h \in \mathbb{R}$, and $\tilde\rho_j = \rho_j + h$. Then

$$
S(\tilde\rho) = S(\rho) + h\Big(\sum_{\circ j}\Phi_j - \sum_{j\circ\!\mid\!\circ k} 2\theta^*_{jk}\Big),
$$

where the first sum is taken over all faces j. The second sum is taken over all interior edges, and j and k are the faces on either side. Clearly, the functional S cannot have a critical point unless the term in brackets vanishes. Hence, the functional S is scale invariant if and only if

$$
\sum_{\circ j}\Phi_j = \sum_{j\circ\!\mid\!\circ k} 2\theta^*_{jk}, \tag{9}
$$

and this is a necessary condition for the existence of a critical point. If equation (9) is not satisfied, then, under the gradient flow, all radii $r = e^\rho$ will either tend to zero or grow without bound. If, on the other hand, equation (9) is satisfied, so that S is scale invariant, then one may restrict the search for critical points to the set $\{\rho \mid \sum \rho_j = 0\}$.

Using equation (2) one sees that the second derivative of S is the quadratic form

$$
S'' = \sum_{j\circ\!\mid\!\circ k} \frac{\sin\theta_{jk}}{\cosh(\rho_k-\rho_j) - \cos\theta_{jk}} (d\rho_k - d\rho_j)^2,
$$

where the sum is taken over all interior edges. Hence $S'' > 0$ unless $d\rho_j = d\rho_k$ for all pairs j, k of faces.

The following theorem summarizes the above results.

Theorem 1 ([BS02]). *A function ρ on the faces gives the logarithmic radii of a circle pattern with given data if and only if it is a critical point of the functional $S(\rho)$.*

The functional $S(\rho)$ is strictly convex on the set $\{\rho \mid \sum \rho_j = 0\}$. Critical points are hence minima. If a circle pattern exists for given data, it is unique up to similarity.

The question whether a circle pattern *exists* for given cellular decomposition, intersection angles, and boundary conditions is more delicate. One has to show that $S \to \infty$, if $\|\rho\| \to \infty$ while $\sum \rho_j = 0$. For a treatment of this problem, the reader is referred to [BS02].

For practical purposes, it may be sufficient to check the existence of a specific circle pattern experimentally. Indeed, if a circle pattern does *not* exist for given data, then some of the ρ will tend to $\pm\infty$ under the gradient flow. Conversely, if a numerical minimizer succeeds in approximating a minimum of $S(\rho)$, then this is a strong indication that the corresponding circle pattern really exists; especially if the radii do not differ greatly in magnitude and if they do not change much if the accuracy of the calculation is increased.

The functional $S(\rho)$ is so constructed that each partial derivative $dS/d\rho_j$ is the difference between the actual value of the total angle subtended by the neighboring circles and its nominal value of Φ_j, which is 2π for interior circles; see equation (8). Hence, if a numerical minimizer finds a solution ρ at which the gradient of $S(\rho)$ is almost zero, then the circles will fit together almost exactly when the pattern is reconstructed.

Currently, the method of choice to practically construct circle patterns seems to be Thurston's algorithm as developed further and implemented by Stephenson [Thu, DS95]. Basically, it consists in adjusting, iteratively, the radius of each circle so that the neighboring circles (whose radii are fixed for the moment) fit around. This is equivalent to minimizing, iteratively, the functional $S(\rho)$ in each coordinate direction.

5 Examples

The circle patterns shown in figures 1(b) and 1(c) were created using the *Mathematica* software. It provides an implementation of the polylogarithms, but the evaluation is slow. Thus an `InterpolatingFunction` approximating Clausen's integral was computed once and for all from equation (10), and then formula (11) was used to compute the dilogarithm. The boundary conditions were chosen such that the outer intersection points lie on the sides of an equilateral triangle.

The circle patterns shown in figures 3, 4, and 6 were created using the *Java Tools for Experimental Mathematics*, which are currently being developed at the Sonderforschungsbereich 288 [Sfb].

Figure 3 shows three circle patterns with square grid combinatorics and

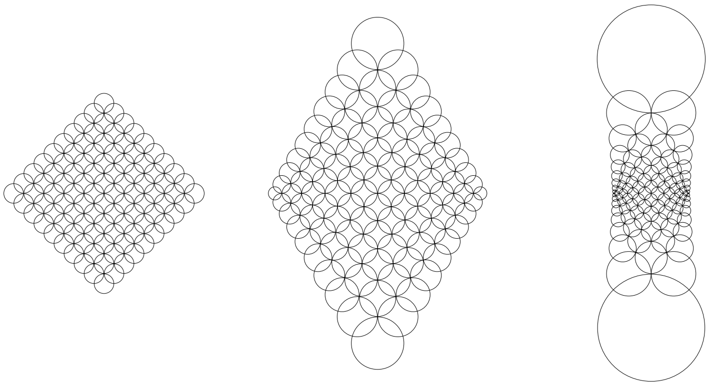

Fig. 3. Square grid combinatorics. $\theta = \pi/2$.

intersection angles $\pi/2$. The boundary conditions are given by $\Phi = 3\pi/2$ for all boundary circles except the ones in the corners, for which $\Phi = \pi$ for the pattern on the left, $\Phi = 5\pi/6$ and $7\pi/6$ for the pattern in the middle, and $\Phi = \pi/2$ and $3\pi/2$ for the pattern on the right.

Figure 4 shows circle patterns with hexagonal combinatorics. All intersection angles are $\theta = 2\pi/3$. The boundary conditions were chosen such that the outer intersection points lie on the sides of a triangle. The triangle for the pattern on the right is degenerate. It has two right angles and one angle is zero.

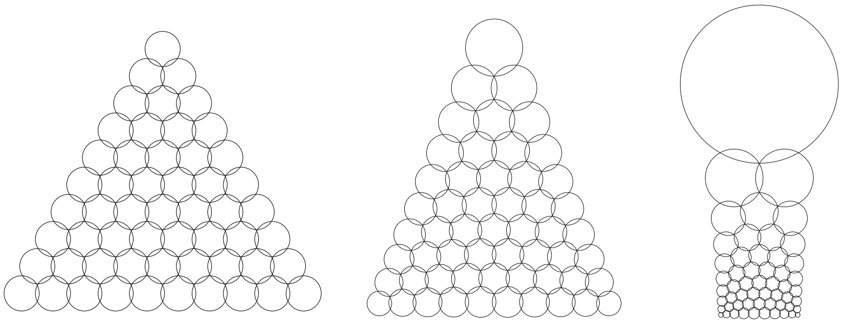

Fig. 4. Hexagonal combinatorics. $\theta = 2\pi/3$.

We have been considering circle patterns in which the vertices of the cellular decomposition correspond to intersection points of circles. Thus, it is required that the intersection angles θ sum to 2π around each vertex. Often, a different type of pattern is considered, in which all vertices have three edges but the angles do not necessarily sum to 2π. At least the case where the sum is greater than 2π can be reduced to the type considered in this paper by adding circles as shown in figure 5(a). The angles for the new edges (see figure

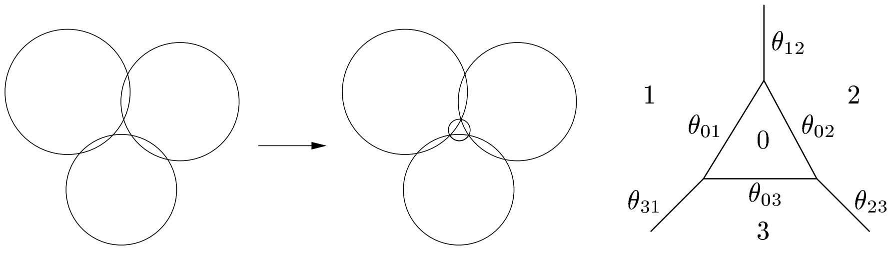

(a) (b)

Fig. 5. Adding circles if $\sum \theta_{jk} > 2\pi$ around a vertex.

5(b)) are determined by the equations

$$\begin{aligned} \theta_{12} + \theta_{20} + \theta_{01} &= 2\pi \\ \theta_{23} + \theta_{30} + \theta_{02} &= 2\pi \\ \theta_{31} + \theta_{10} + \theta_{03} &= 2\pi. \end{aligned}$$

Hence $\theta_{01} = \pi - \frac{1}{2}(\theta_{12} - \theta_{23} + \theta_{31})$, etc. (Note that even if the condition $\theta_{12} + \theta_{23} + \theta_{31} > 2\pi$ is not satisfied, one may get values for $\theta_{01}, \theta_{02}, \theta_{02}$ which lie in the correct range $0 < \theta < \pi$. In this case, however, the circle pattern does not exist and the functional does not have a minimum.)

The circle patterns of figure 6 were constructed in this way. They are similar to those of figure 4. But here the intersection angles are $\theta = 3\pi/4$.

6 The numerical evaluation of the functional

How useful is the functional $S(\rho)$ for the practical construction of circle patterns? This depends primarily on how easily it can be computed numerically. Formula (7) is not so useful for this purpose since it involves the complex dilogarithm. However, the imaginary part of the dilogarithm function can be expressed in terms of a 2π-periodic real function, Clausen's integral $\mathrm{Cl}_2(x)$. It can be defined by the imaginary part of dilogarithm on the unit circle:

$$\mathrm{Cl}_2(x) = \operatorname{Im} \mathrm{Li}_2(e^{ix}). \tag{10}$$

From equation (4), its Fourier expansion is seen to be

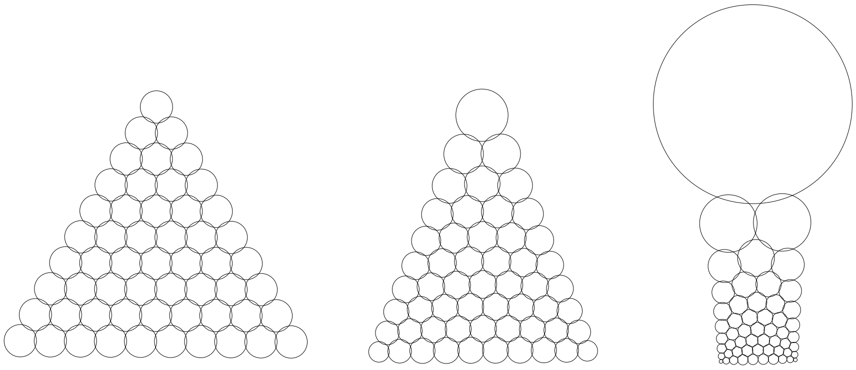

Fig. 6. Hexagonal combinatorics. $\theta = 3\pi/4$.

$$\mathrm{Cl}_2(x) = \sum_{k=1}^{\infty} \frac{\sin kx}{k^2}.$$

Substituting $\zeta = e^{i\xi}$ in equation (5), one obtains for $0 \leq x \leq 2\pi$ the equation

$$\mathrm{Cl}_2(x) = -\int_0^x \log\left(2\sin\frac{\xi}{2}\right) d\xi.$$

The imaginary part of the dilogarithm function is expressed in terms of Clausen's integral by the equation

$$\mathrm{Im}\,\mathrm{Li}_2(e^{x+i\theta}) = \varphi x + \frac{1}{2}\,\mathrm{Cl}_2(2\varphi) - \frac{1}{2}\,\mathrm{Cl}_2(2\varphi + 2\theta) + \frac{1}{2}\,\mathrm{Cl}_2(2\theta), \qquad (11)$$

where $\varphi = f_\theta(x)$. If one wants to calculate the functional $S(x)$, the following formula is even more useful:

$$\mathrm{Im}\,\mathrm{Li}_2(e^{x+i\theta}) + \mathrm{Im}\,\mathrm{Li}_2(e^{-x+i\theta}) = px + \mathrm{Cl}_2(\theta^* + p) + \mathrm{Cl}_2(\theta^* - p) - \mathrm{Cl}_2(2\theta^*),$$

where $\theta^* = \pi - \theta$ and

$$p = 2\arctan\left(\tanh\left(\frac{x}{2}\right)\tan\left(\frac{\theta^*}{2}\right)\right). \qquad (12)$$

Clausen's integral $\mathrm{Cl}_2(x)$ was implemented in the following way using Chebyshev approximation. The function

$$h(x) = -\log\left(2\sin\frac{x}{2}\right) + \log x$$

is analytic at $x = 0$ and

$$\mathrm{Cl}_2(x) = \int_0^x h(\xi)\, d\xi - x(\log x - 1).$$

The function $h(x)$ was approximated in the interval from $-\pi$ to π by a Chebyshev series. This series was then integrated. The algorithms for fitting, integrating and evaluating Chebyshev series which were used are described in [PTVF92].

In principle, the evaluation of Clausen's integral is not more complicated or expensive than the evaluation of a trigonometric or exponential function. Note that, with p as in equation (12), $f_\theta(x) = \frac{1}{2}(\theta^* + p)$ and $f_\theta(-x) = \frac{1}{2}(\theta^* - p)$. Hence, when computing $S(\rho)$, the simultaneous computation of the gradient is (almost) free.

References

[Brä92] W. Brägger. Kreispackungen und Triangulierungen. *Enseign. Math.*, 38:201–217, 1992.

[BS02] A. I. Bobenko and B. A. Springborn. Variational principles for circle patterns and Koebe's theorem. `arXiv:math.GT/0203250`, March 2002.

[CdV91] Y. Colin de Verdière. Un principe variationnel pour les empilements de cercles. *Invent. Math.*, 104:655–669, 1991.

[DS95] Tomasz Dubejko and Kenneth Stephenson. Circle packing: experiments in discrete analytic function theory. *Experiment. Math.*, 4(4):307–348, 1995.

[HBS+99] M. K. Hurdal, P. L. Bowers, K. Stephenson, et al. Quasi-conformally flat mapping the human cerebellum. In C. Taylor and A. Colchester, editors, *Medical Image Computing and Computer-Assisted Intervention—MICCAI '99*, volume 1679 of *Lecture Notes in Computer Science*, pages 279–286, Berlin, 1999. Springer.

[Lei01] G. Leibon. Characterizing the Delaunay decompositions of compact hyperbolic surfaces. `arXiv:math.GT/0103174`, March 2001.

[PTVF92] William H. Press, Saul A. Teukolsky, William T. Vetterling, and Brian P. Flannery. *Numerical recipes in C.* Cambridge University Press, Cambridge, second edition, 1992.

[Riv94] I. Rivin. Euclidean structures of simplicial surfaces and hyperbolic volume. *Ann. of Math.*, 139:553–580, 1994.

[RS87] B. Rodin and D. Sullivan. The convergence of circle packings to the Riemann mapping. *J. Differential Geom.*, 26:349–360, 1987.

[Sch97] O. Schramm. Circle patterns with the combinatorics of the square grid. *Duke Math. J.*, 86(2):347–389, 1997.

[Sfb] Sfb 288. Java tools for experimental mathematics. `http://www-sfb288.math.tu-berlin.de/~jem` (to appear).

[Thu] W. P. Thurston. The geometry and topology of three-manifolds. Electronic version 1.0 of 1997 currently provided by the MSRI under `http://www.msri.org/publications/books/gt3m/`.